AFRL-SR-AR-TR-09-0362

REPORT DOCUMENTATION PAGE

PLEASE DO NOT RETURN YOUR FORM TO THE ABOVE ORGANIZATION.

1. REPORT DATE *(DD-MM-YYYY)*	2. REPORT TYPE	3. DATES COVERED *(From - To)*
24Sep2009	FINAL REPORT	From 1Jul07 to 30Dec08

4. TITLE AND SUBTITLE
(DURIP FY07) SPATIALLY-RESOLVED SYSTEM FOR POLARMETRIC MEASUREMENTS AT SUBWAVELENGTH SCALES

5a. CONTRACT NUMBER
FA9550-07-1-0524

5b. GRANT NUMBER
07NE254

5c. PROGRAM ELEMENT NUMBER

6. AUTHOR(S)
Dr. Aristide Dogariu

5d. PROJECT NUMBER

5e. TASK NUMBER

5f. WORK UNIT NUMBER

7. PERFORMING ORGANIZATION NAME(S) AND ADDRESS(ES)
UNIV OF CENTRAL FLORIDA
SCHOOL OF OPTICS/CREOL
4000 CENTRAL FLORIDA BLVD, POBOX 162700, Orlando, FL 32816-2700

8. PERFORMING ORGANIZATION REPORT NUMBER

9. SPONSORING/MONITORING AGENCY NAME(S) AND ADDRESS(ES)
AF OFFICE OF SCIENTIFIC RESEARCH
875 NORTH RANDOLPH STREET ROOM 3112
ARLINGTON VA 22203

10. SPONSOR/MONITOR'S ACRONYM(S)

11. SPONSOR/MONITOR'S REPORT NUMBER(S)

12. DISTRIBUTION/AVAILABILITY STATEMENT
DISTRIBUTION STATEMENT A: UNLIMITED

13. SUPPLEMENTARY NOTES

14. ABSTRACT

This proposal will purchase an Aurora-3 Near-Field Scanning Optical Microscope (NSOM) that has the capability of high, sub-wavelength spatial resolution, improved focusing mechanism, dual-light path design, and accurate probe-to-sample patented measuring capability making it the most advanced NSOM available. The proposed instrumentation offers superior performance in near-field optical characterization and contrast mechanisms with the high resolution of scanning probe microscopy techniques. The acquisition of this equipment will allow the PI to expand greatly his capability in 3D polarimetry. There is also a great promise to pursue nano-designs of photonics-based technologies with this NSOM.

15. SUBJECT TERMS
Photonic Crystal Interface Waveguide Circuit, Waveguide Technology, Antimonide Superlattice

16. SECURITY CLASSIFICATION OF:			17. LIMITATION OF ABSTRACT	18. NUMBER OF PAGES	19a. NAME OF RESPONSIBLE PERSON
a. REPORT	b. ABSTRACT	c. THIS PAGE			Dr. Aristide Dogariu
					19b. TELEPHONE NUMBER *(Include area code)* 4078236839

Spatially-resolved system for polarimetric measurements at subwavelength scales

Submitted by:
Dr. Aristide Dogariu
School of Optics/CREOL
University of Central Florida

submitted to:
Air Force Office of Scientific Research
PIE/DURIP
875 North Randolph Street
Suite 325, Room 3112
Arlington, VA 22203-1768

Summary

The instrumentation developed under this DURIP award is a near-field optical scanning system which can operate in both active-illumination and passive-collection modes and will assist in a variety of fundamental studies on polarimetry of optical near fields and novel developments in applied photonic sensing.

This instrumentation complements the existing facilities and offers unique capabilities to expand our research and explore the temporal and spatial evolution of subwavelength electromagnetic phenomena, which could lead to new approaches for optical sensing.

The addition of this near-field scanning instrumentation is necessary for developing detailed knowledge about the properties of 3D optical fields. The system will also assist in designing, characterizing, and controlling photonic probes which can directly couple all three components of the field under test and then re-emit the radiation. The selected state-of-the-art measurement system adds to the existing research capabilities within the College of Optics and Photonics; currently, three graduate students are involved in projects utilizing the unique capabilities of this instrumentation.

Research Instrumentation

Figure 1 shows a schematic of the MultiView 4000 (MV4000). The near-field scanning apparatus consists of two tip piezo scanners and a sample piezo scanner which are integrated into an Olympus BX-51 microscope. The setup is placed on a vibration isolation stage which is critical to minimize vibrations and thus measure high quality scans.

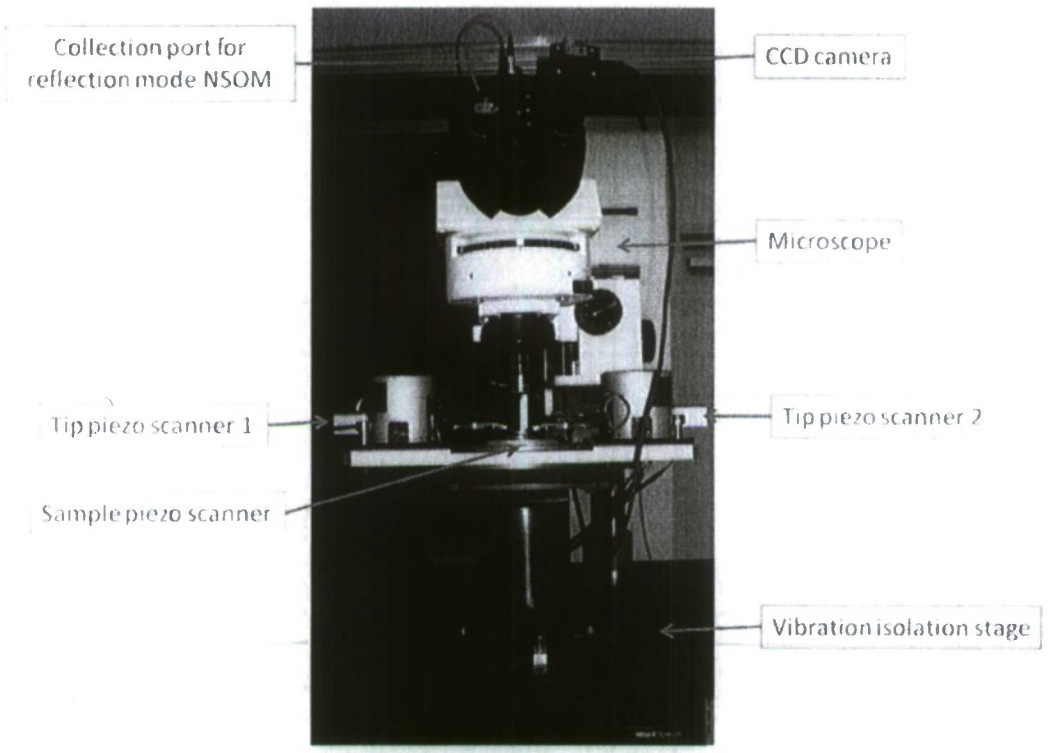

Fig. 1: Main components of MV4000.

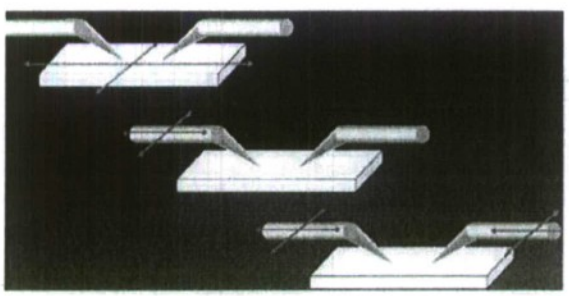

In our current configuration we may scan with either one probe or two as shown here. However the system may be upgraded to incorporate up to four probes.

The tips manufactured by Nanonics may be brought to within subwavelength separations as shown in Fig. 2 (10-200 nm depending on the tip), opening up a number of possibilities to test energy transfer and field correlations in real time over subwavelength distances.

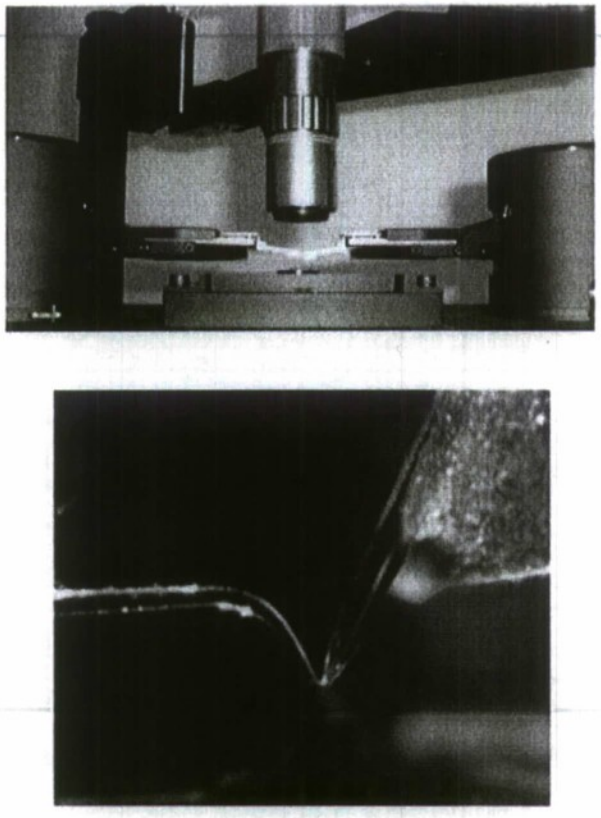

Fig. 2: Two tips brought close together on MV 4000.

Scanning may be done with either the tips or the sample. Lateral and vertical scanning may be controlled separately, allowing the user to scan in the XY plane with the either the sample or the tip(s) and scan in the Z direction with either the sample or the tip(s). This allows the user, for example, to keep the tips in a fixed lateral location in the focal plane of the microscope objective while independently following the topography or allows a scan to be completed with one tip while another one is fixed.

The hardware is run with a code written in LabVIEW. This code has the ability to run user defined scans and interfacing with other LabVIEW modules, giving the user tremendous flexibility to automate scans which extend far beyond traditional scanning of a single area. In addition, the tip may be brought in and out of contact during a scan or moved laterally over a range of 85 μm during a scan.

Technical Features

The specifications of the selected instrumentation include the following unique capabilities.

1) Sample piezo scanner: x, y, z sample scanner (85 x 85 x 85 μm) with 24 mm central opening can accommodate samples up to 34 mm for standard operation. Central opening allows for thick or unconventional geometries to be scanned. 5 mm rough sample movement range with a resolution of 0.25 μm.

2) Two tip piezo scanners: x, y z tip scanner (30 x 30 x 30 μm) with x, y, z rough tip movement range (5 x 5 x 10 mm). x, y, z rough positioning resolution (0.25 x 0.25 x 0.065 μm). Ability to bring two probes together with a separation of as little as 10 nm. Can upgrade to maximum of four tip piezo scanners.

3) Image resolution: x, y, z while scanning (<0.15 x <0.15 x <0.05 nm).

4) Feedback operation: tuning fork normal-force operation, up to 100 kHz frequency range with 10 V maximum driving amplitude.

5) Tip enhanced Nano Photonics Module (TEN module): individual placement of tip and sample relative to microscope objective.

6) Olympus BX-51 upright microscope comprising long working distance 10x (NA 0.25) and 50x (NA 0.45) objectives and c-mount port.

7) CCD camera mounted into eyepiece with 1280 x 1024 pixels and a pixel size of 5.2 x 5.2 μm. Communication: USB 2.0.

8) Minus-k portable vibration isolation platform: ultra-low natural frequencies and requires no air supply

9) Nanonics Supertips probes:

    a. Cr coated AFM probes with 20 nm aperture. Option of standard, deep trench, or with gold or silver nanoparticles on tip.

    b. NSOM probes with apertures down to 50 nm and Cr-Au coated. Option of standard or deep trench probes. Choice of single mode, multimode or polarization maintaining fiber. 15 mW maximum CW input power.

    c. Micropipette probes with either hallow aperture for nano-writing of liquids or fabricated into a coaxial probe, thermocouple or thermal resistive junction.

Tips can also be made liquid cell compatible.

10) Liquid cell: ability to image live cells in buffer solution. 12 mm clear aperture holder.

11) Software: LabVIEW based, supports several imaging modes including AFM (contact and non-contact), phase, error signal, and NSOM. Can read up to 8 channels simultaneously. Image size continuously variable from 2 x 2 to 1024 x 1024 with multiple z. Features AUX data acquisition, image and line profiles displayed in real time, intuitive scan parameter setup, and ability to customize by

user or interface with other LabVIEW modules allowing the user significant versatility to collect data and design tests beyond standard imaging.

12) Ability to scan with either one or two probes simultaneously (can upgrade to up to four probes). Independent control of lateral and vertical scanning which may be controlled with either probe or sample.

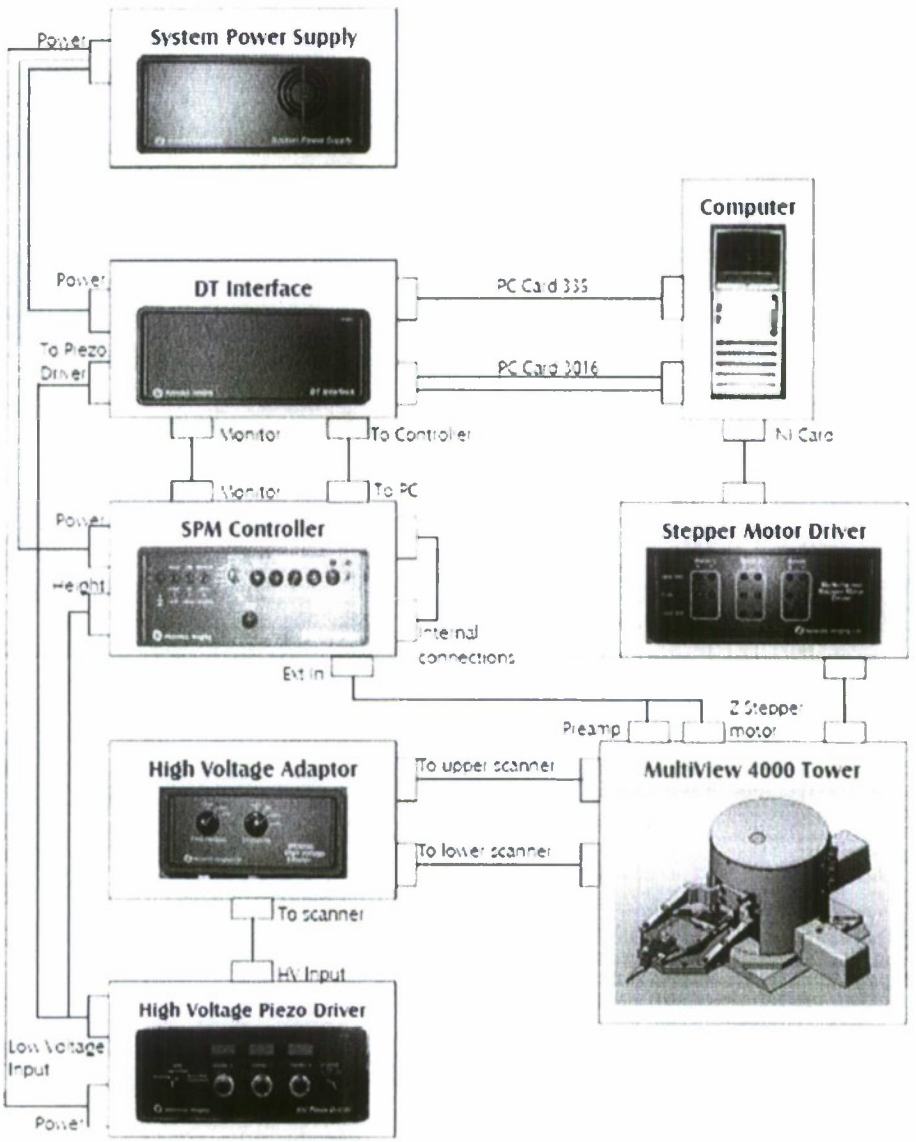

Fig. 3: Main components of MultiView 400 system

MultiView 4000 Tower

The parts of the MultiView 4000 tower are shown in the diagram below:

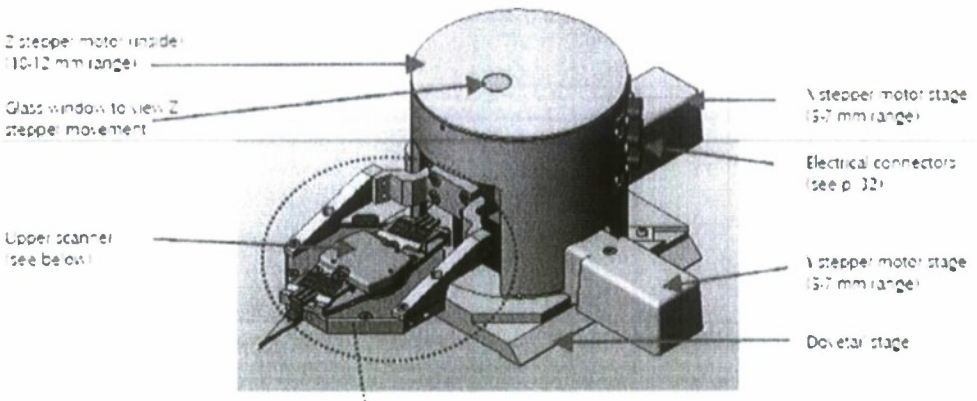

Upper Scanner

Each tower houses an upper scanner, as shown below:

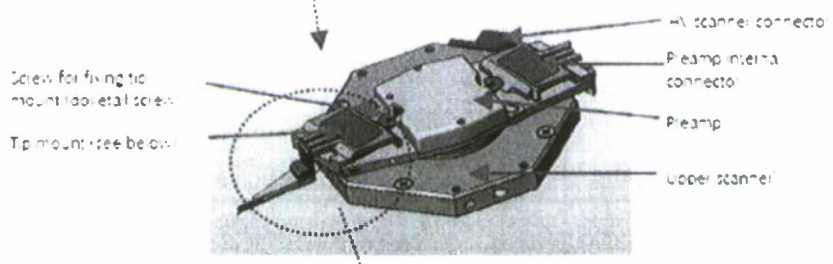

Tip Mount

The MultiView 4000 tip mount is shown below.

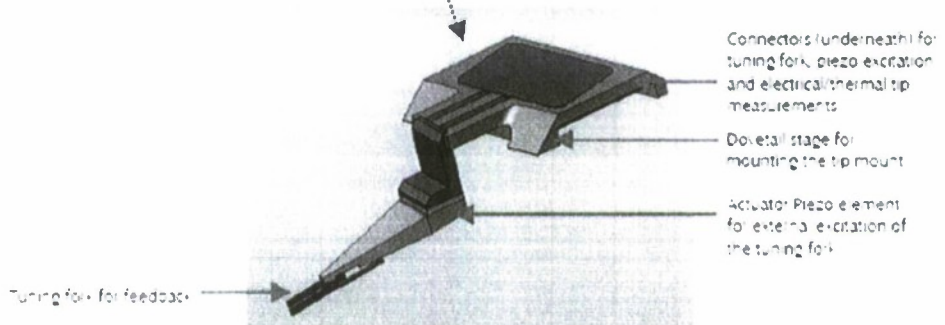

Fig. 4: Main components of MultiView 400 scanning tower

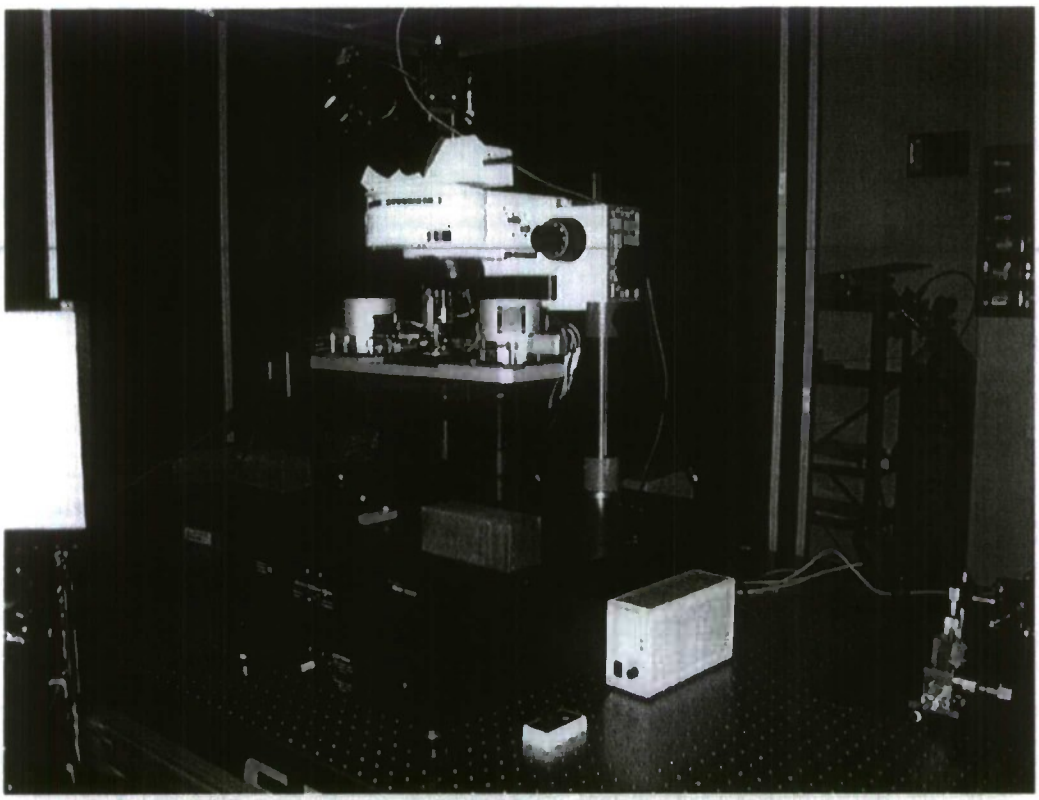

Fig. 5: Picture of the MV 4000 installed in the PI's laboratory

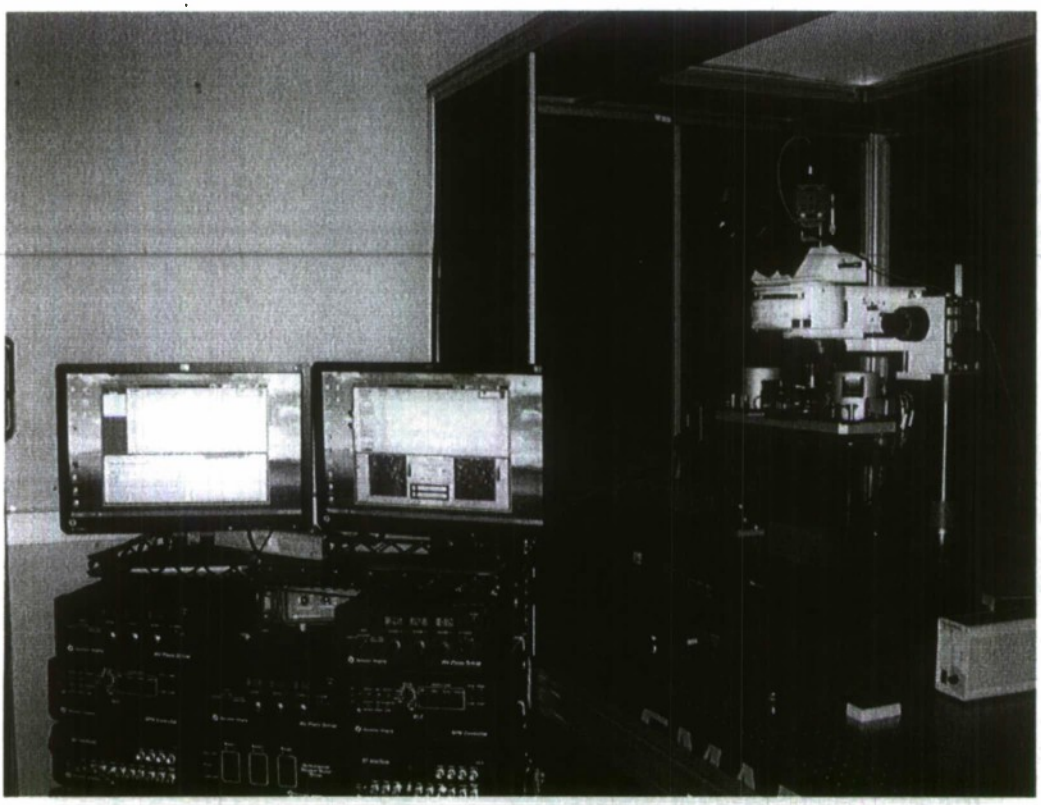

Fig. 6: Picture of the dual NSOM system installed in the PI's laboratory, including the MV 4000 and the associated controls

Modes of Operation

i) Tip based illumination

In the tip illumination mode, the incoming laser beam is directed towards sample through the fiber-tip. Signal reflected from the sample is collected in the far field. Currently only reflection mode is set up, but system can be easily upgraded to integrate transmission mode or a combination of both reflection and transmission modes.

Reflection Tip-illuminated reflection mode allows nanoscale optical imaging of opaque and non-transparent samples, by collecting the reflected light and directing it to the signal detector.

Tip-illuminated polarization imaging Due to the flexible system, it is easy to achieve optical activity/polarization studies with additional wave plates or other user provided components within the existing stage-detection geometry, e.g., synchronous configuration of dual detectors for parallel and perpendicular collection.

ii) Tip-based collection

Non-contact topography is achieved with normal-force feedback and tuning-fork technology.

Collection-based achieved by collecting light emerging from the sample through a fiber probe. Can collect light from a far field source, from a second probe or from light emitted and recollected by a single probe.

Polarization collection can also be achieved with additional wave plates or other user-provided components within the existing stage-detection geometry, e.g., a synchronous configuration of dual detectors for parallel and perpendicular collection.

Fluorescence collection can be obtained with appropriately sensitive detector and correctly placed filters within the existing optical path.

This instrumentation incorporates the ability to record multiple optical signals allowing us to simultaneously collect, for example, a far field reflection mode image with the light reflected back from the tip or light reflected back from one tip and also collected in a second tip and correlate those images to the sample topography.

With the variety of probes that have been designed for this system coupled with the flexibility to program user-defined scans, the ability to simultaneously but independently scan with multiple probes or the sample and the ease with which the system may be upgraded, allows the user a veritable cornucopia of near-field measurement possibilities.

Projects supported by the research instrumentation

A number of projects are currently in progress using this research instrumentation. These projects involve performing near-field tomographic reconstruction, measuring low refractive index contrast materials, measuring the polarimetric response of near fields interacting with a sample, and measuring live cells in physiologically relevant conditions. Some details are provided bellow.

Near field tomography:
The fields from an NSOM scan penetrate a finite depth into the material, giving one the ability to see structures below the surface of a sample. Reports have been published in the literature showing that materials can be imaged below a transparent surface. Determining how deep the structure is below the surface, however, has not been well addressed in the literature. This may be accomplished using tomographic reconstruction, which requires knowledge of both the amplitude and the phase of the collected light.

One way to accomplish this is to simultaneously illuminate and collect light with the same probe. In this way, light that is reflected from the end of the tip (E_{rt}) interferes with light that is emitted from the tip, reflects off the sample and is subsequently recollected (E_{rs}), as is shown schematically in Fig 7(a). By measuring this interference as a function of tip to sample separation, the phase may be extracted and thus the *local* thickness of the film may be determined. By repeating this measurement at many points across the sample, a map of the underlying topography may be extracted.

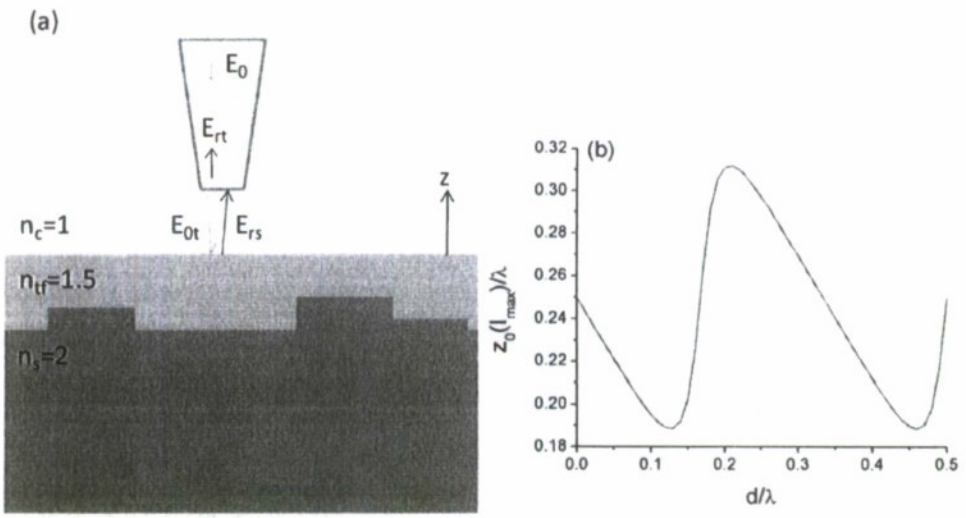

Fig. 7: (a) Schematic of near field tomography experiment. (b) Closest tip to sample separation resulting in a maximum of measured intensity.

The sample we are interested in exploring is the reconstruction of the topographical variations in a substrate that has been coated with a thin transparent film,

as shown in Fig. 7(a). In this case, the sample may be modeled as a three layer system which is excited by a dipole and with a detector placed in the far field above the sample surface. The closest tip to sample separation that results in a peak of measured intensity is given by the result shown in Fig. 7(b). From this figure we can see that the problem is ill-posed (multiple film thicknesses will give a maximum measured intensity for the same tip-sample separation). This may be resolved if the range of film thickness is known *a priori* or if another measurment is performed, for example at another wavelength or angle or with another probe.

In Fig. 8 we show AFM topography scans of the samples that will be used in this experiment. These samples consist of a thin layer (~100 nm) of SiO2 deposited on Si. From these scans, we can see that the topopgraphy is very smooth (peak to peak variation of less than 6 nm) over the entire scan range. We can also see the excellent images of very flat samples produced by this instrumentation.

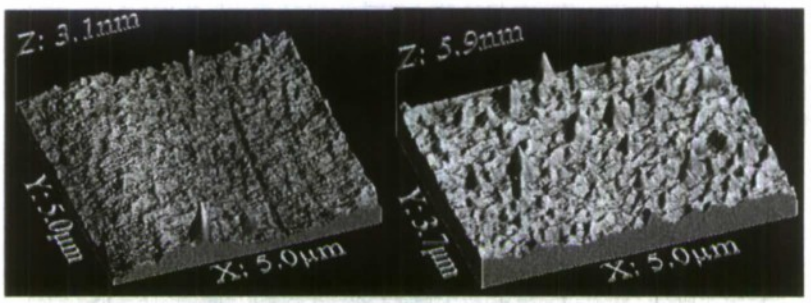

Fig. 8: Test of the AFM capability: image of ~100 nm of SiO_2 deposited on Si

Imaging of low refractive index contrast materials:
Photothermal refractive (PTR) glasses are glasses which, with proper treatment, undergo changes that result in a change in the refractive index of the material, while still exhibiting high transparency and low scattering. This treatment allows to user to locally change the refractive index of the glass, resulting in a roughly 10^{-4} index contrast of the bulk material between unexposed and exposed regions. This may be used, for example, to fabricate gratings.

This small refractive index contrast is introduced into the material by causing the nucleation of nanoparticles in the glass. This treatment causes the refractive index to change but also results in a significant increase in the level of scattering. Several techniques have been developed to reduce this level of scattering, but it is not known if this scattering has been reduced to the theoretical limit. Currently the only way to analyze these particles is to allow them to grow large enough to be seen in a conventional microscope, particles which are much larger than what is used for making these gratings. However, the NSOM may image even smaller particles than conventional microscopy, opening the door to potentially analyze properly developed glasses.

Near-field Stokes polarimetry

The optical near field intensity maps from NSOM measurements are derived from contributions both from the local morphological structure and the local optical properties of the sample. A polarimetric treatment of optical fields reveals information about these properties. Hence, a near field polarimetric analysis can offer insight into the local behavior of material systems. This polarimetric characterization is commonly achieved through Stokes polarimetry, a technique relying on four polarimetric intensity measurements: horizontal, vertical, 45°, and circular polarizations.

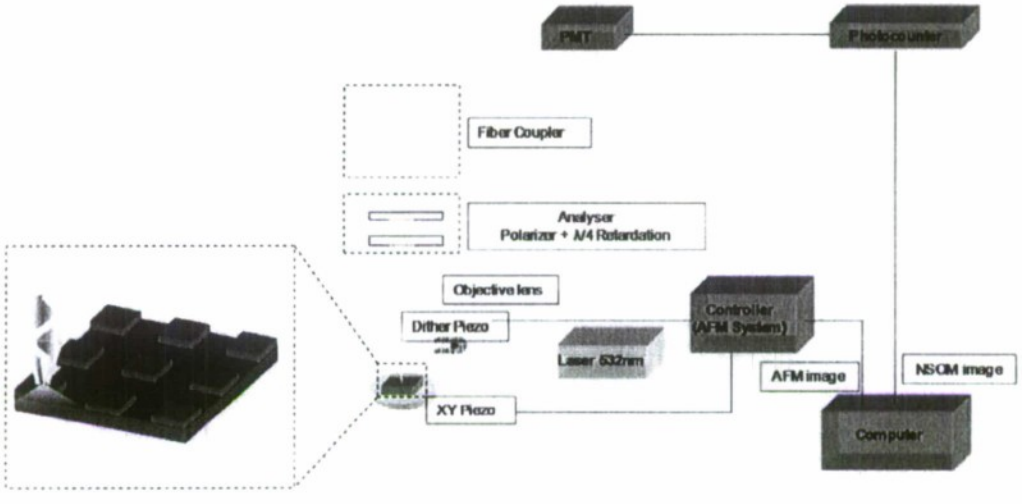

Figure 9: Schematic of Stokes polarimetry setup.

A schematic of the setup is shown in Fig 9. We measured a complete Stokes vector measurement in reflection mode NSOM. The test object consisted of a U-shaped periodic pattern made of homogeneous gallium phosphide (GaP) which is isotropic and has a refractive index of 3; as such the polarimetric changes are entirely determined by the object shape and the complex interaction with the optical near fields. In order to determine the Stokes vector distribution, we performed four separate scans (each time recording a different polarization state) over the same area with dimensions 5 μm by 5 μm, obtaining both an intensity distribution together with the corresponding AFM topographical map.

Figure 10 shows a map of the reconstructed two dimensional polarization ellipse is superimposed onto the AFM measured topography. We observe that the polarization state is sensitive to topographical changes independent of changes in the material refractive index.

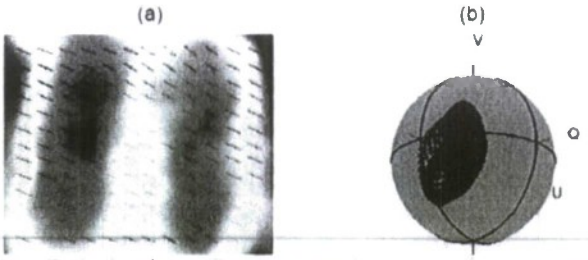

Fig. 10: (a) Polarization State mapping on the topography after optimization process. The black and green colors indicate handedness. (b) Poincare sphere with indicated Stokes vectors.

Liquid cell imaging of live biological cells:

One of the holy grails of near field imaging is to image live cells in physiologically relevant conditions. This system provides a number of technical challenges which must be overcome in order to successfully image and manipulate live cells using near field probes. Overcoming these challenges however will open to the door to perform several important experiments. For example, many structures in cells are too small to be resolved using conventional imaging; however they are the right size to be resolved using an NSOM. In addition we can study energy transfer over distances on the order of 100-1000 nm.

Imaging of living cells has already been experimentally demonstrated, but the implementations that have been reported in the literature prevent the user from bringing two probes close together to study energy transfer and other similar effects. We are currently working with Nanonics to design a liquid cell setup that will overcome this limitation and allow the user to perform multiprobe experiments of living cells.

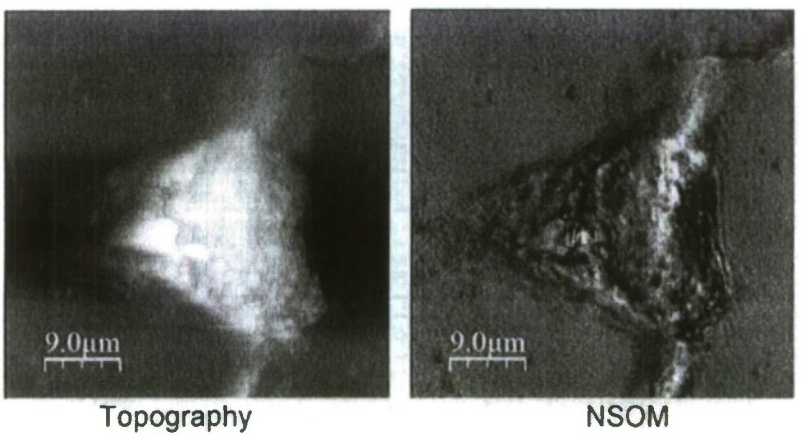

Fig. 11: Image of NT2 cells taken in our lab

Publications supported by the research instrumentation:

[1] J. Bae, D. Haefner, S. Sukhov, A. Dogariu, *Full Stokes Polarimetry In the Near Field*, accepted for oral presentation, COSI 2009.

[2] D. C. Kohlgraf-Owens, D. Haefner, S. Sukhov, A. Dogariu, *Sub-Surface Interferometric Near-Field Tomography*, accepted for oral presentation, COSI 2009.

AFOSR Nanoelectronics, award no. FA9550-06-1-0270
Title: A multispectral detector based on arrays of carbon nanotubes.
PI: Paola Barbara, Georgetown University
Final report for the period April 1 2006 – June 30 2009

This project focused on studying carbon nanotube quantum dots under terahertz irradiation for potential applications as detectors in the frequency range 0.3-10 THz. The basic physical principle is photon assisted tunneling. A carbon nanotube of finite length has a discrete energy spectrum and can be described as a one-dimensional quantum well. The length of the well is typically the distance between the source and drain electrodes attached to the nanotube. A voltage applied to a nearby gate electrode shifts the Fermi energy in the nanotube by capacitively inducing charges and populating or depleting the energy levels in the nanotube quantum dot. Here we consider the case in which the source and drain electrodes are weakly coupled to the nanotube and a substantial charging energy is necessary to add an electron to the dot. In this case, the current as a function of gate voltage will show sharp peaks corresponding to resonant elastic tunneling of electrons, one at a time, occurring when the Fermi energies of the leads are aligned with an energy level in the dot. Coulomb blockade occurs between the peaks and the voltage interval between adjacent peaks is characterized by the energy level spacing and the charging energy of the dot. When an electromagnetic field is present, transport can also occur via photon assisted tunneling, that is inelastic tunneling with absorption or emission of photons. Photon assisted tunneling generates side peaks in the Coulomb blockade regions: the voltage interval between the side peak and the main peak is determined by the photon energy ($h\nu \cong 4$ meV at 1 THz) and the height of the side peaks is related to the intensity of the electromagnetic field. Carbon nanotubes are ideal quantum dots for photon assisted tunneling in the THz range, because their typical charging energy ($E_C \sim 10$ meV or larger for lengths smaller than a micron) is quite large, allowing detection of side peaks up to a few terahertz at power levels on the order of femtowatts. The lower frequency that can be detected is comparable to the width of the peaks, which depends on the temperature and on characteristic quantum dot properties, such as the coupling between the nanotube and the leads.

Reports of photon-assisted tunneling in quantum dots are scarce [1] and the effect is largely unexplored. This is mainly due to the difficulty to efficiently couple THz radiation to the devices ad the limited availability of powerful THz sources. The goals of our AFOSR supported research were:

1) Design and construction of a variable temperature probe (300K-2K) coupled to a tunable THz source;
2) Fabrication of carbon nanotube quantum dots and quantum dot arrays;
3) Testing quantum dot response to THz radiation as a function of temperature and frequency.

Goals 1) and 2) were accomplished. Goal 3) is still in progress.

Once reliable detection from carbon nanotube quantum dots is obtained, it will be used to detect THz signals with spectral resolution, as well as to fabricate on-chip detectors to test possible operation of carbon nanotube multiple quantum wells as quantum cascade laser THz sources. Below we describe in detail the accomplishments towards goals 1) and 2) and our progress on goal 3).

Experimental setup

We purchased and tested a BWO source that is tunable in the range 100-180 GHz. The output from this source is coupled to a frequency doubler and a tripler, to achieve tunable frequency in the ranges 200-350 GHz and 600-1000 GHz. The power output at 1000 GHz is about 0.1 mW, two orders of magnitude smaller than a typical laser source. We designed and built a low-temperature probe with optical access through a polished stainless steel waveguide (center tube in Fig. 1.). THz radiation is guided from the source to the waveguide using a 45° reflective mirror, mounted at the top of the probe. The sample needs to be carefully aligned to the focal point of a lens, which is mounted in the cold stage.

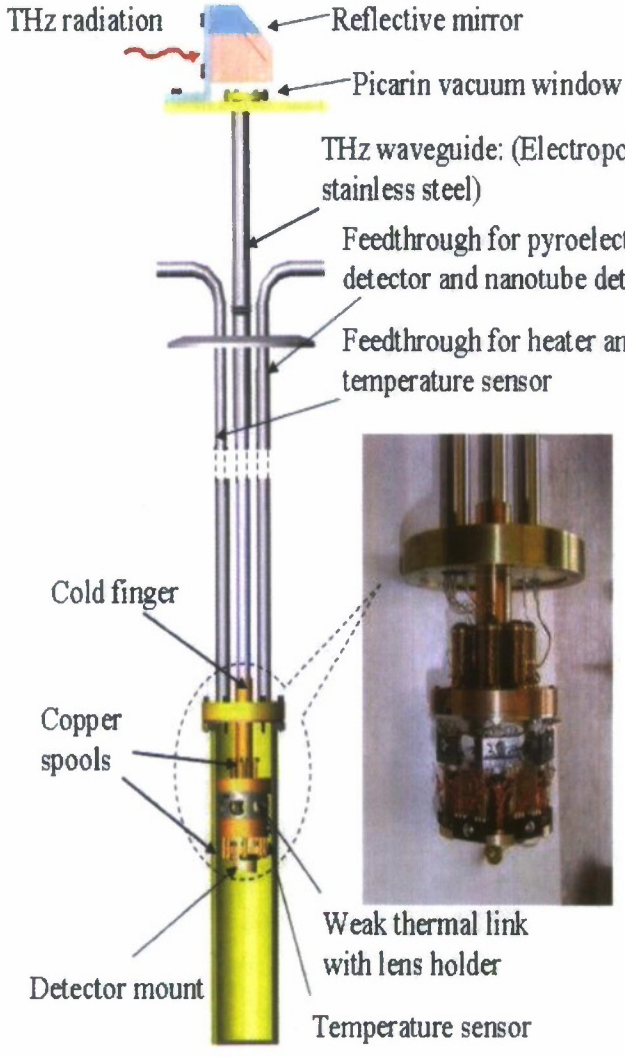

Fig.1. Schematic of our home-made low temperature probe.

Although our probe is a low-cost optical cryogenic system, it requires careful alignment of each sample with respect to the focusing lens mounted in the cold stage. This means that only one chip with a few nanotubes clustered in a small area can be measured for every cooldown. Fig. 2 shows a picture of the actual experimental set-up.

We note that we recently received an AFOSR/DURIP award to purchase a cryostat with optical windows that can operate from room temperature to 3 K without the use of liquid helium. This cryostat will certainly speed up sample testing, because optical windows provide easier alignment between samples and THz source, and will also eliminate expenses associated with liquid helium consumption.

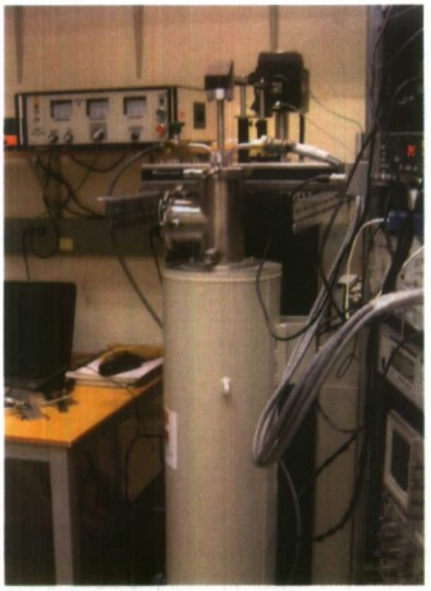

Fig.2. Image of the actual set-up, including the low-temperature probe (see Fig. 5) and the THz source.

Sample fabrication and characterization

A field emission scanning electron microscope with e-beam lithography was acquired and installed at Georgetown University in the Summer 2006, following a NSF/MRI award (PI: P. Barbara). We have developed device patterning and alignment techniques and started fabricating carbon nanotube transistors ranging from 100 nm to 1 μm.

The nanotubes are grown by chemical vapor deposition from patterned catalyst islands and source and drain electrodes are patterned using both e-beam lithography, for submicron features, and shadow masks for larger contact pads. The source and drain electrodes are formed by sputtering thin films (50 nm) of palladium or niobium. In our first quantum dot design, the doped silicon substrate, capped with 500 nm of silicon dioxide, is used as a gate electrode.

We characterized nanotube junctions from room temperature to 2K. The energy levels in the quantum dots were determined by measuring differential conductance of the devices as a function of gate and source-drain voltage, as shown in Figs. 2 and 3, and all the nanotube junctions showing quantized energy levels have been tested under exposure to THz radiation. Our THz source can be tuned in a wide frequency range (100-180 GHz, 200-350 GHz and 600-1000 GHz) and the exposure to THz radiation is controlled by an optical chopper. The signal from the chopper is fed as a reference to the lock-in amplifier, which is used for the differential conductance measurements of the junctions. Although our samples are qualitatively very similar to the samples measured in ref. [1] and show good quantum dot behavior, all the samples we tested so far did not show a measurable response to THz radiation. This can be explained considering that our THz source is two orders of magnitude weaker than the laser source used in the detection experiment in ref. [1]. Moreover, even though the source used in ref. [1] was quite powerful, only few samples showed a response [2], indicating that the reliability of the response is still an unsolved issue.

Progress on improving coupling to THz radiation

This past year we focused on optimizing the coupling between the THz field and the CNT quantum dots according to the following plan:

- Change device design to include on-chip antennas to improve coupling with THz radiation.
- Use more powerful laser sources to better test coupling with different antenna designs.
- Use top electrodes as local gates to create tunable barriers in the dot and obtain arrays of tunable quantum dots with individual side gates, to explore photon assisted tunneling as a function of quantum dot parameters.
- Measure response as a function of temperature and frequency.

We worked on the first three points and fabricated new samples that are ready to be tested at low temperature.

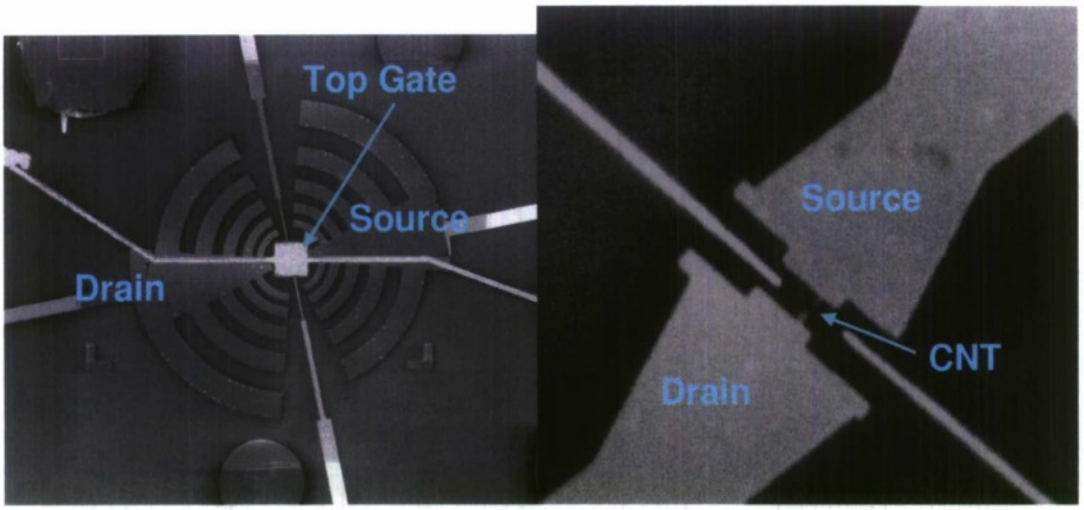

Fig. 3: Left: Log periodic antenna design to operate in the frequency range 700 GHz to 2.5 THz. The antenna was patterned by e-beam lithography and liftoff of 100 nm thick sputtered Gold. Right: Enlarged area showing the source and drain electrodes connected to the carbon nanotube before the deposition of the top electrode. The distance between the source and drain electrodes is about 400 nm.

In addition to high reflection losses, due to the mismatch between the detector impedance and the free space impedance, the dimension of the effective detection region (which is comparable to the size of the quantum dots, about ~ 300 nm) is much smaller than the radiation wavelength (300 microns at 1 THz in free space), as well as the region in which the THz power can be focused (~ 5 mm^2). **On-chip antennas** therefore are necessary to couple the low-power THz radiation to carbon nanotube devices. Antennas will significantly increase the effective detection area and will reduce impedance mismatch. Since we plan to test the device response as a function of frequency, we select antenna designs that work in a wide frequency range. Planar self-complementary antennas [3] are good candidates because their impedance is frequency independent and close to the impedance of free space (within about a factor of two). One example is shown in Fig. 3, where we patterned electrodes as log-periodic antennas [4], designed to operate in the frequency range 700 GHz to 2.5 THz. For these samples the substrate is intrinsic silicon and the gate electrodes will be patterned either on the side of the nanotube or on the top, after growing a SiO_2 layer or Al_2O_3 layer on top of the device.

We plan to test these antennas coupled to the nanotubes with a **more powerful laser source.** We recently started a collaboration with Prof. Dennis Drew at the University of Maryland. The laser lines available in his laboratory and their corresponding power output are listed in the table below.

CO_2 pumped Laser Lines Available at UMD

Frequency (THz)	FIR Gas	FIR Output ~ (mW)
7.2	CD_3OH	8
6.9	CD_3OH	8
5.3	CH_3OD	21
4.3	CH_3OH	12
3.1	CH_3OH	30
2.5	CH_3OH	50
2.3	CH_3OH	10
1.5	CH_3NH_3	5

Lower frequencies can be obtained by providing additional gases. For example, a 1.28 THz line can be obtained by purchasing CH_2F_2.

The laser will be coupled to the sample (which is at liquid helium temperature) either by using the low temperature probe built in our laboratory or a cryostat with optical windows available in Prof. Drew's laboratory. We already adapted this cryostat to mount carbon nanotube quantum dots on the sample stage. A Winston cone is mounted behind the optical window to focus THz radiation on the on-chip antenna (see Fig. 4).

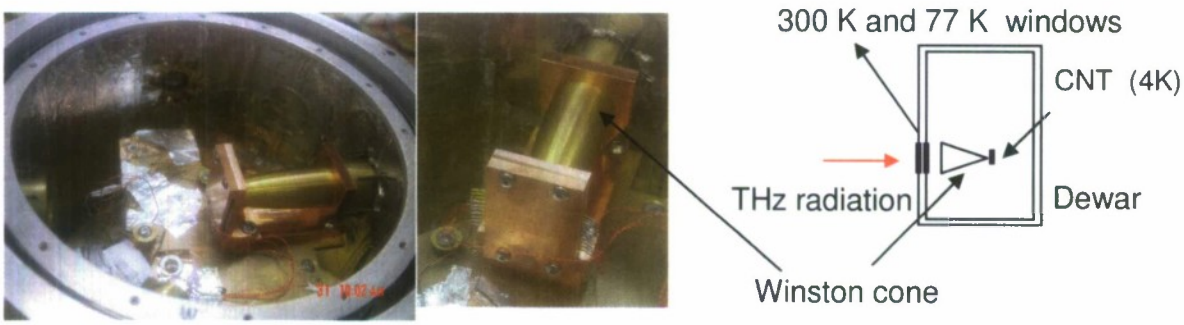

Fig. 4: Mounting of the CNT device for illumination with THz radiation. A Winston cone as used to concentrate the beam on device area. This configuration will also reduce the possibility of optical misalignment considerably. Each polyethylene window has ~ 85 % transmittance below 20 THz.

As we mentioned earlier, we also changed the design of the quantum dots connected to the antennas. We previously tested quantum dots with the doped silicon substrate used as a backgate and the length of the quantum dot defined by the distance between source and drain electrodes. Although these devices have a simpler fabrication procedure (no gate electrode needs to be patterned) and show good quantum dot behavior, **new quantum dot designs need to be developed**. The use of a doped silicon substrate instead of intrinsic silicon will substantially change the performance of the on-chip antenna. We started using substrates made of intrinsic silicon. In this case, we pattern small top gate

that cover just the quantum dot area or small side gates (see Fig. 3). The top gates are patterned after depositing an insulating layer on the device. We tested several options for the insulating layer, including PECVD deposition of SiO_2 in our laboratory or ALD of Al_2O_3 at the Nanocenter at the University of Maryland. Several tests showed that the ALD process is best suitable for fabrication of carbon nanotube quantum dots. Testing of the new samples is ongoing.

References

[1] Y. Kawano, S. Toyokawa, T. Uchida and K. Ishibashi, *THz photon assisted tunneling in carbon-nanotube quantum dots*, Journal of Applied Physics **103**, 034307-034310 (2008).

[2] Dr. Koji Ishibashi, private communication.

[3] Y. Mushiake, *Self-complementary antennas,* IEEE Antennas and Propagation Magazine, **34**(6), 23–29, 1992.

[4] R. H. DuHamel & D. E. Dummel, *Broadband Logarithmically periodic antenna structures*, IRE International Convention Record, vol. 5, pp. 119-128, (1957).